Localized electronic states around stacking faults in silicon carbide

Hisaomi Iwata,[1] Ulf Lindefelt,[1,2] Sven Öberg,[3] and Patrick R. Briddon[4]
[1]Department of Physics and Measurement Technology, Linköping University, SE-581 83 Linköping, Sweden
[2]ABB Corporate Research, SE-721 78 Västerås, Sweden
[3]Department of Mathematics, Luleå University of Technology, SE-971 87 Luleå, Sweden
[4]Department of Physics, University of Newcastle upon Tyne, Newcastle NE1 7RU, United Kingdom
(Received 8 October 2001; published 28 December 2001)

We report on a first-principles study of all the structurally different stacking faults that can be introduced by glide along the (0001) basal plane in 3C-, 4H-, and 6H-SiC based on the local-density approximation within the density-functional theory. Our band-structure calculations have revealed that both types of stacking faults in 4H-SiC and two of the three different types of stacking faults in 6H-SiC give rise to quasi-two-dimensional energy band states in the band gap at around 0.2 eV below the lowest conduction band, thus being electrically active in *n*-type material. Although stacking faults, unlike point defects and surfaces, are not associated with broken or chemically perturbed bonds, we find a strong localization, within roughly 10–15 Å perpendicular to the stacking fault plane, of the stacking fault gap state wave functions. We find that this quantum-well-like feature of certain stacking faults in SiC can be understood in terms of the large conduction-band offsets between the cubic and hexagonal polytypes. Recent experimental results give qualitative support to our results.

DOI: 10.1103/PhysRevB.65.033203 PACS number(s): 71.23.An, 71.15.−m

SiC is a promising material for high-power, high-frequency, and high-temperature applications. Three of the most popular polytypes, 3C-, 4H-, and 6H-SiC, have attracted considerable attention during the past decades since their special material properties are very much suitable for such applications. However, there are still material problems that need to be investigated and understood in order to fully develop SiC-based technology. One such problem is the occurrence of stacking faults (SF). In general, the SF energy of SiC is believed to be small (around 3 and 15 mJ/m^2 for 6H- and 4H-SiC, respectively) compared to other semiconductors such as Si (55 mJ/m^2), diamond (280 mJ/m^2), or GaAs (45 mJ/m^2).[1–3] Due to the small SF energy it is relatively easy to develop extended SF regions in SiC crystals, which, if electrically active, can seriously affect the device performance. However, both theoretical and experimental studies of SF in SiC are very limited.[1–4] In this paper, we report on a first-principles supercell band-structure calculation for the 3C-, 4H-, and 6H-SiC polytypes with and without SF. Our theoretical calculations have revealed that SF in SiC can actually give rise to electrically active states in the band gap, whose wave functions are strongly localized perpendicular to the SF plane.

A mechanism for the creation of SF is the motion of partial dislocations (here we consider only dislocations of the glide set), which leave behind an imperfect crystal containing a SF. The easy slip plane in the hexagonal SiC polytypes is the basal (0001) plane, and complete dislocations in the basal planes are usually dissociated into two partials according to the Burgers vector reaction formula[1,2,5]

$$a/3\langle 2\bar{1}\bar{1}0\rangle \rightarrow a/3\langle 1\bar{1}00\rangle + a/3\langle 10\bar{1}0\rangle, \tag{1}$$

where a is the lattice constant in the basal plane. For example, 3C-SiC has the stacking sequence $\ldots(ABC)(ABC)(ABC)\ldots$ where A, B, and C denote bilayers as shown in Fig. 1. The propagation of a partial dislocation (which induces the change $A\rightarrow B$, $B\rightarrow C$, and $C\rightarrow A$) gives rise to the faulted sequence $\ldots(ABC)|(BCA)(BCA)\ldots$, where $|$ denotes the slip or SF plane. As will be discussed later, partial dislocations may introduce several different nonequivalent types of SF into the noncubic SiC polytypes.

The computational method is based on the local-density functional theory, and the properties of SF are modeled using a supercell approach. The wave functions are expanded in a basis containing *s*-, *p*-, and *d*-symmetry Gaussian orbitals, and the charge density is described in a plane-wave basis. The method gives analytical expressions for forces on atoms and uses norm-conserving pseudopotentials and nonlinear core corrections. Since the supercells are extended along the *c* axis, so that the corresponding first Brillouin zone is almost two dimensional (2D), the Brillouin zone integration is replaced by a summation over six special Monkhorst-Pack *k* points on the basal plane of the Brillouin zone. In order to determine *ab initio* lattice constants for the perfect crystals, we employed supercells containing 24 atoms for perfect 3C-, 4H-, and 6H-SiC, i.e., the supercells for 3C-, 4H-, and 6H-SiC consist of 4, 3, and 2 primitive unit cells, respectively (3C-SiC is treated as hexagonal with 6 atoms per unit cell).

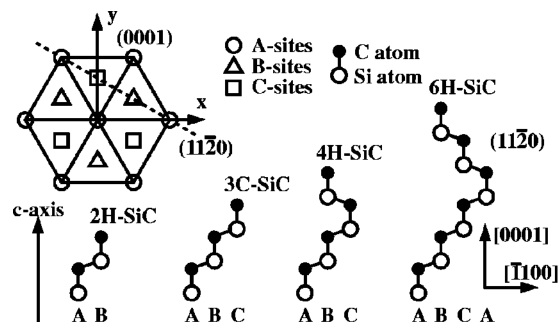

FIG. 1. Stacking sequences of the hexagonal layers in four common SiC polytypes.

 ©2001 The American Physical Society

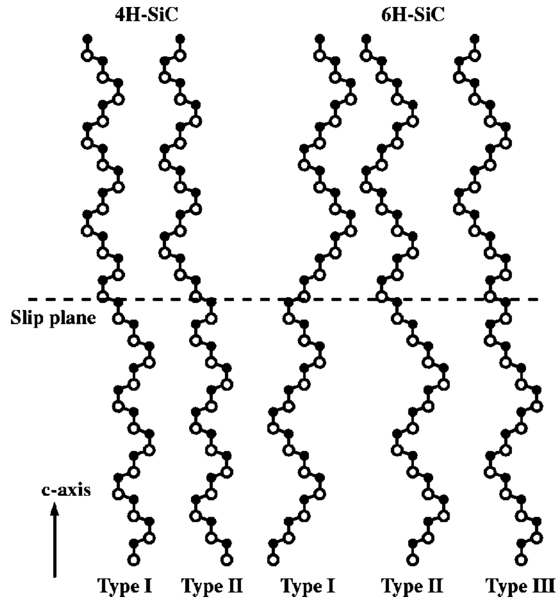

FIG. 2. Geometrically distinguishable SF in 4H- and 6H-SiC. Type I and type II SF are related through an interchange of Si and C atoms.

Not only the lattice constants a and c, but also all atomic positions in the supercell, have been optimized to minimize the total energy (intrasupercell relaxation).

In order to investigate the electronic structure of SF, we calculate the Kohn-Sham band structures of both perfect and faulted crystals, using supercells containing 96 atoms in both cases. It is preferable to employ the same size of the supercell for all polytypes when calculating the total energies or when comparing other results for different polytypes, since cancellations of systematic errors are expected to some extent. For example, the 96-atom supercell for perfect 4H-SiC can be expressed by the stacking sequence $(ABAC)_{12}$ and hexagonal translation vectors $\mathbf{a}_1=(a,0,0)$, $\overline{\mathbf{a}}_2=(-a/2, a\sqrt{3}/2,0)$, $\overline{\mathbf{a}}_3=(0,0,c)$, where, in this case, c is 12 times the corresponding lattice constant for the primitive unit cell. This supercell thus contains 12 primitive cells stacked on top of each other, while the corresponding supercells for 3C- and 6H-SiC contain 16 and 8 primitive unit cells, respectively. To be able to treat faulted crystals with the same size and geometry of the supercell as for perfect crystals, we modify the vector $\mathbf{a}_3$. Thus, instead of $\mathbf{a}_3$ we use $\mathbf{a}_3'=(-a/2,a\sqrt{3}/6,c)$ or $\mathbf{a}_3''=(a/2,-a\sqrt{3}/6,c)$, depending on whether the SF corresponds to $A\rightarrow B$ etc. or $A\rightarrow C$ etc. Furthermore, we have found that 96-atom supercells are sufficient to avoid artificial SF-SF interactions.

An inspection of the arrangement of atoms obtained when introducing SF in different glide planes in the SiC unit cells gives that the 3C-, 4H-, and 6H- polytypes have 1, 2, and 3 geometrically different SF, respectively, as shown in Fig. 2. (When determining the number of different SF that can be introduced by pure glide, it should be noted that the space group for 4H- and 6H-SiC, i.e., C_{6v}^4, is nonsymmorphic: a 180° rotation around the c axis is to be followed by a translation by $c/2$.) We will refer to them as type I in 3C-SiC, type I and II in 4H-SiC, and as type I, II, and III in 6H-SiC.

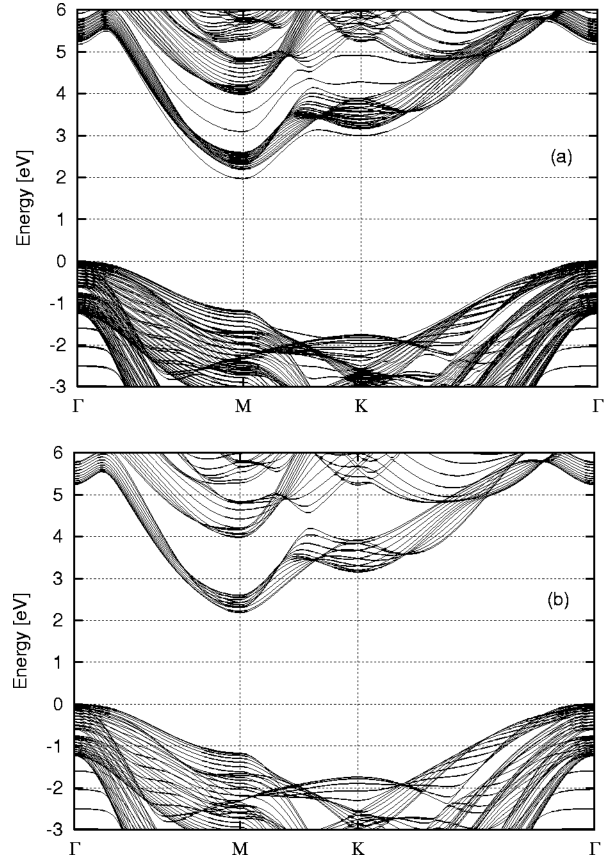

FIG. 3. Band structures of 4H-SiC (a) with and (b) without SF of type I.

Since the first Brillouin zone is almost 2D, we calculate the Kohn-Sham eigenvalues along the high symmetry lines Γ-M, M-K, and K-Γ. In the 96-atom supercell calculations for faulted crystals we employ lattice parameters a and c determined theoretically using 24-atom supercells. However, we have determined the effect of intrasupercell atomic relaxations on the band structure also for 4H-SiC with SF, i.e., the position of each atom in the supercell was optimized until the Hellmann-Feynman forces vanished. We found that such relaxation effects have negligible influence on the band-structure energies. Since the intrasupercell relaxation for 96-atom supercells is very time consuming, we have not performed such relaxations for faulted 3C- and 6H-SiC, i.e., each atomic coordinate in the c direction is ideal.

Figures 3(a) and 3(b) show the Kohn-Sham band structures for 4H-SiC with and without SF of type I. When comparing Figs. 3(a) and 3(b), a SF-induced band (split-off band) can be observed around 0.2 eV below the conduction-band minimum at the M point of perfect 4H-SiC. To clarify the nature of this band, we plot in Fig. 4 the function

$$f(z)=\int\int|\Psi_M(x,y,z)|^2 dx\, dy, \qquad (2)$$

where Ψ_M is the wave function at the M point and the integration for each value of z along the c axis is performed in the basal plane within the supercell. Figure 4(a) shows $f(z)$ for the lowest conduction band in perfect 4H-SiC. It is

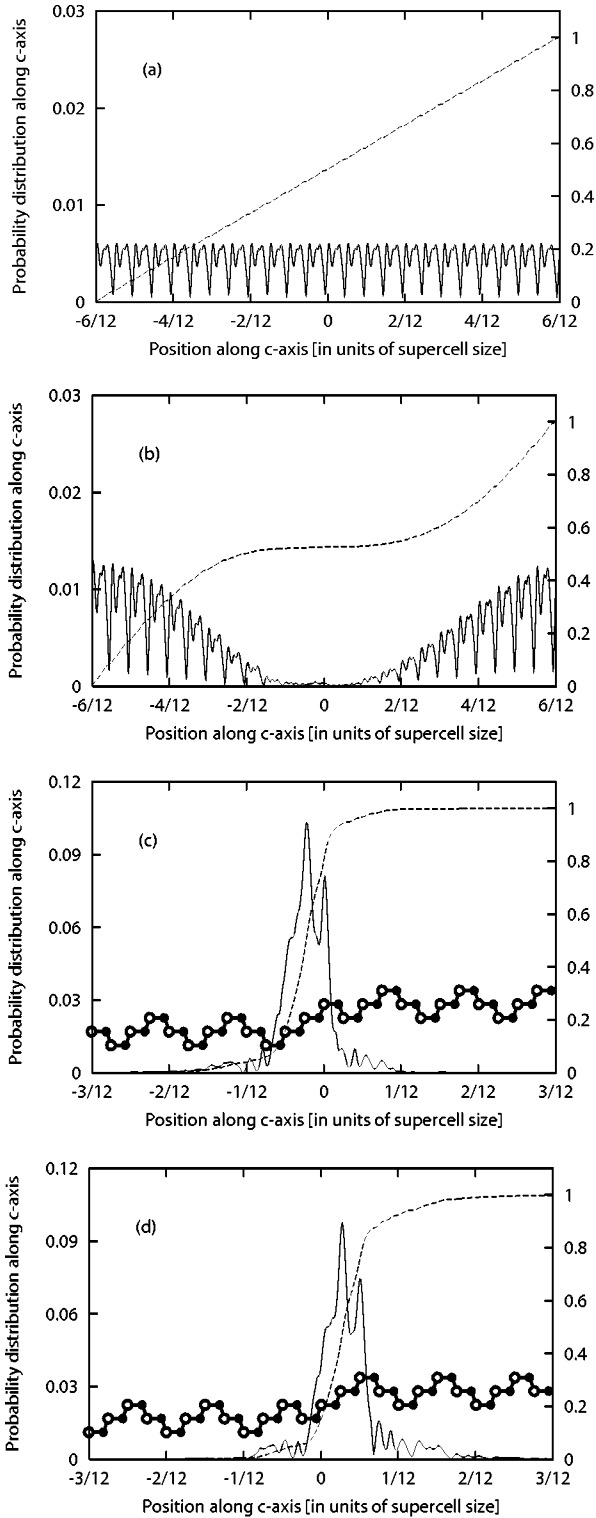

FIG. 4. The function in Eq. (2) for the wave function at the *M* point of (a) the lowest conduction band in perfect 4H-SiC, (b) the lowest conduction band above the split-off band in 4H-SiC with SF of type I, (c) the localized SF band (i.e., the split-off band) in 4H-SiC with SF of type I, and (d) the localized SF band in 4H-SiC with SF of type II are shown. The normalization integral $I(z)$ defined in Eq. (3) is also shown (right-hand scale), together with the corresponding stacking sequences.

TABLE I. Positions of the localized SF band minima (in eV) below the conduction-band minima at the *M* point

	3C-SiC	4H-SiC	6H-SiC
Type I	~0	0.22	0.17
Type II		0.18	0.19
Type III			~0

clearly an extended state. Figure 4(b) shows $f(z)$ for the lowest state above the split-off band in faulted (type I) 4H-SiC. This is clearly also an extended state, but with a distinct influence from the SF. In contrast, Figs. 4(c) and 4(d), which are for the split-off band in 4H-SiC with SF of type I and type II, respectively, show a clear localization in the direction perpendicular to the glide plane. The degree of localization is further demonstrated in Fig. 4 by the normalization integral

$$I(z)=\int^{z} f(z')dz', \tag{3}$$

starting the integration at the bottom of the supercell. Thus, both SF in 4H-SiC lead to a localized SF band in which the electron has an enhanced probability to move in the immediate vicinity (within around 10 Å) of the SF.

By comparing band structures of perfect and faulted crystals for all the polytypes 3C, 4H, and 6H, we have found that both SF in 4H-SiC and the SF of type I and II in 6H-SiC give rise to strongly localized band states in the band gap. Furthermore, the SF in 3C-SiC and the type III SF in 6H-SiC also give rise to states that show signs of localization around the SF plane. The difference is that in these two cases the degree of localization is clearly smaller than for type I and II SF gap states in 4H- and 6H-SiC, and the corresponding states are very close to the valence-band maximum (3C and 6H) and the conduction-band minimum (6H), rather than clearly separated from the extended band states. The situation for the energies is summarized in Table I.

The type I and type II SF bands in the gap for 4H- and 6H-SiC are rather strongly localized, within 10–15 Å, perpendicular to the glide plane. This localization is thus possible without the involvement of deformed, broken, or chemically perturbed bonds, which give rise to localized states around, for instance, point defects, dislocations, and surfaces. To shed some light on the localization mechanism, we note from Figs. 4(c) and 4(d) that the localized wave functions have most of their amplitude in the region where the stacking sequence is more 3C-like (straight). It has been found[6] that for a 3C-4H or 3C-6H interface, the conduction-band offsets are around 1 and 0.7 eV, respectively, with the conduction band for 3C-SiC being below that for 4H- (6H-) SiC, whereas the corresponding valence-band offsets are much smaller. Therefore, if there are 3C-like regions in faulted 4H- or 6H-SiC crystals, the conduction electrons tend to be attracted to a region with a locally lower conduction band (like in quantum wells). It is noticeable that the result that the SF of type III in 6H-SiC does not give rise to strongly localized and relatively deep energy states in the

band gap can be explained by this interpretation. The SF of type III does not create a 3C-like sequence in 6H-SiC, but rather a 2H-like (zigzag) sequence, at the same time as the lowest conduction band for 2H-SiC is higher than that for 6H-SiC.[6]

The qualitative correctness of our results is confirmed in two papers by Takahashi *et al.*[7] By growing 4H- and 6H-SiC crystals using different growth directions, crystals containing a small number of SF ($<10\ \mathrm{cm}^{-1}$) or a large number of SF ($10^2-10^4\ \mathrm{cm}^{-1}$) could be produced. The resistivity in a direction essentially perpendicular or parallel to the SF planes was then measured, both for *n*-type and *p*-type samples. It was found that in *n*-type samples of both 6H and 4H polytypes the resistivity perpendicular to the SF was much larger than that along the SF at low temperatures, much larger than what can be explained by the "normal" bulk resistivity anisotropy,[8] mainly caused by the anisotropy of the electron effective-mass tensor.[9] Furthermore, no resistivity anomaly was observed in *p*-type samples. No proper explanation of these results could be given.

In view of our results, this resistivity anomaly is quite understandable. In *n*-type samples, the electrons are trapped by the localized SF band, and will essentially remain there at low temperatures. Due to the localization in the *c* direction, the electron transport in the *c* direction is hindered, whereas the electrons are free to move in the SF plane. On the other hand, the Fermi level in *p*-type samples is well below the localized SF band, which is, therefore, not involved in the current transport.

Furthermore, electrical degradation (i.e., an increase in on-state voltage with time) of 4H-SiC pin diodes has been reported.[10] It was found that this degradation coincided with the appearance of structural defects, mainly interpreted as SF in the basal plane, created by a combination of the stress and electron-hole recombination energy. This electrical degradation can now be understood as caused by SF states in the band gap, preventing the build-up of a normal electron-hole plasma in the device.

In summary, we have performed first-principles band-structure calculations for 3C-, 4H-, and 6H-SiC with and without SF. The calculations were performed for all structurally different SF that can be obtained by pure glide. It was found that the SF of type I and type II in 4H- and 6H-SiC give rise to strongly localized, electrically active states in the band gap, even though no broken or chemically perturbed bonds are involved, much like for a quantum well. An interpretation of these phenomena in terms of the large conduction-band offsets between the cubic and hexagonal polytypes considered here has been suggested, and recent experimental results[7,10] firmly indicate the existence of such localized electrically active SF bands in the band gap of both 4H- and 6H-SiC.

The authors gratefully acknowledge financial support from the Swedish Foundation for Strategic Research (SSF), as well as the National Supercomputer Center (NSC), Sweden, for computer time.

[1] M. H. Hong, A. V. Samant, and P. Pironz, Philos. Mag. A **80**, 919 (2000).
[2] K. Maeda, K. Suzuki, S. Fujita, M. Ichihara, and S. Hyodo, Philos. Mag. A **57**, 573 (1988).
[3] P. Käckell, J. Furthmüller, and F. Bechstedt, Phys. Rev. B **58**, 1326 (1998).
[4] M. Y. Chou, M. L. Cohen, and S. G. Louie, Phys. Rev. B **32**, 7979 (1985).
[5] P. Pirouz, Mater. Sci. Forum **264-268**, 399 (1998).
[6] F. Bechstedt, P. Käckell, A. Zywietz, K. Karch, B. Adolph, K. Tenelsen, and J. Furthmüfler, Phys. Status Solidi B **202**, 35 (1997).
[7] J. Takahashi, N. Ohtani, M. Katsuno, and S. Shinoyama, J. Cryst. Growth **181**, 229 (1997); Mater. Sci. Forum **264-268**, 25 (1998).
[8] M. Schadt, G. Pensl, R. P. Devaty, W. J. Choyke, R. Stein, and D. Stephani, Appl. Phys. Lett. **65**, 3120 (1994).
[9] H. Iwata, K. M. Itoh, and G. Pensl, J. Appl. Phys. **88**, 1956 (2000); H. Iwata and K. M. Itoh, J. Appl. Phys. **89,** 6228 (2001).
[10] J. P. Bergman, H. Lendenmann, P. Å. Nilsson, U. Lindefelt, and P. Skytt, Mater. Sci. Forum **353-356**, 299 (2001).